Infrared multiphoton dissociation of 1,2-dichloroethyltrifluorosilane

ARTICLE *in* APPLIED PHYSICS B · NOVEMBER 2009

Impact Factor: 1.86 · DOI: 10.1007/s00340-009-3596-7

Appl Phys B (2009) 97: 625–633
DOI 10.1007/s00340-009-3596-7

Applied Physics B
Lasers and Optics

Infrared multiphoton dissociation of 1,2-dichloroethyltrifluorosilane

P.V. Koshlyakov · P.S. Dementyev · S.R. Gorelik · E.N. Chesnokov · A.K. Petrov

Received: 16 March 2009 / Revised version: 16 May 2009 / Published online: 5 June 2009

Abstract Infrared multiphoton absorption and dissociation of 1,2-dichloroethyltrifluorosilane molecules under the action of pulsed TEA CO_2 laser were experimentally studied. The composition of dissociation products was analyzed. The only products of dissociation have been found to be stable molecules: chloroethylene and trifluorochlorosilane. Dissociation proceeds via chlorine atom transfer from carbon to silicon. The silicon isotope-selective infrared multiphoton dissociation was performed at different wavelengths of the CO_2-laser radiation. High degrees of silicon isotope separation have been achieved.

PACS 82.50.Bc · 82.30.Lp · 31.15.Ew

1 Introduction

In the past decade, the interest in the applications of isotopically pure silicon materials for semiconductor technology has been growing worldwide, in particular, after the thermal conductivity of highly enriched ^{28}Si had been found to be almost 60% higher than that of naturally abundant Si at room temperature [1]. Subsequently, this result was redefined: it was found that the enhancement of the thermal conductivity was about 10% at room temperature, whereas at low temperatures the thermal conductivity of isotopically pure Si exceeds that of the naturally abundant Si by a factor of 8 [2]. This makes it relevant to study the infrared multiphoton dissociation (IR MPD) of silicon-containing molecules in order to find the most appropriate compounds for the laser-induced silicon isotope separation technology.

Silicon has three stable isotopes with the natural composition: 92.22% (^{28}Si), 4.69% (^{29}Si), 3.09% (^{30}Si) [3]. Separation of Si isotopes by means of infrared laser radiation has been studied [4–11]. The most impressive results have been achieved in experiments on MPD of the Si_2F_6 species [6–10]. Kamioka et al. [6, 7] reported that the MPD of Si_2F_6 molecules, induced by pulsed CO_2 laser radiation, has revealed significantly higher dissociation efficiency and high isotope selectivity under mild radiation fluences lower than 1 J/cm^2. The enrichment coefficient (selectivity) reached 30 for the ^{30}Si isotope and 6 for the ^{29}Si isotope.

Despite such impressive results, it is not evident that Si_2F_6 might be considered as the best object for the silicon–isotope separation by means of IR MPD. The molecule contains two Si atoms and the rare isotopes are contained mostly in "isotopically mixed" molecules, such as $^{28}SiF_3$–$^{29(30)}SiF_3$. This fact limits the isotopic effect as during the dissociation of these *isotopically mixed* molecules, the ^{28}Si isotope and the rare one (^{29}Si or ^{30}Si), would pass equally into products. In addition, we could expect that the isotopic shift in the molecular vibrational frequencies in the *isotopically mixed* molecules should be less than that in the isotopically *pure* molecules.

P.V. Koshlyakov (✉) · P.S. Dementyev · E.N. Chesnokov · A.K. Petrov
Institute of Chemical Kinetics and Combustion SB RAS, Institutskaya, 3, Novosibirsk 630090, Russia
e-mail: pvk@ns.kinetics.nsc.ru

P.S. Dementyev · E.N. Chesnokov
Novosibirsk State University, Pirogova, 2, Novosibirsk 630090, Russia

S.R. Gorelik
Institute of Material of Research and Engineering, 3, Research Link, Singapore 117602, Singapore

Silicon isotope selective IR MPD of compounds containing single silicon atoms, such as SiH_2F_2 [12], $SiF_3C_6H_5$ [13, 14, 19], SiF_3CH_3 [15, 16], SiF_3CHCH_2 [17], $Si(OCH_3)_4$ [18] was studied previously. The maximum isotope selectivities reached for the IR MPD of these molecules were found to be lower than that for Si_2F_6. From the analysis of spectroscopic and kinetic characteristics of the MPD of these molecules, one can conclude that the main reason for the higher efficiency of the Si_2F_6 MPD is its low dissociation threshold (188 kJ/mol [7]) compared to the other molecules studied [11–19] (around 420 kJ//mol). Therefore, the further search of the compounds should be limited to those containing only one silicon atom and possessing a relatively low dissociation threshold.

Haszeldine et al. [20–24] experimentally studied the thermal decomposition of halogenoalkylsilanes. They showed that the halogenoalkylsilane compounds, in which a halogen atom is present at α- or β-carbon relative to silicon, essentially easily undergo the unimolecular decomposition via the intramolecular rearrangement involving the unimolecular transfer of halogen from carbon to silicon. It was shown that dissociation with the β-halogen atom transfer proceeds via a four-center transition state and leads to the formation of stable products, olefin and halogen-substituted silane:

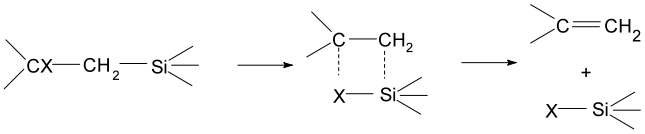

Dissociation energies for these reactions are in the range of 100–160 kJ/mol [20]. A similar transfer of α-halogen proceeds via a three-center transition state and is followed by the formation of halogen-substituted silane and carbene.

The low dissociation energy makes the unimolecular decomposition reactions of halogenoalkylsilanes, proceeding via the halogen atom transfer from carbon to silicon, promising for the isotope selective IRMPD. Recently, the IR MPD of SiF_3CH_2Cl under exposure to CO_2-laser radiation was studied [25]. It has been found that the presence of the chlorine atom at α-carbon significantly improves the characteristics of the silicon isotope-selective dissociation compared with a similar molecule SiF_3CH_3. The disadvantage of SiF_3CH_2Cl for selective IR MPD is that one of its dissociation products is a singlet methylene $^1CH_2$ which is a very reactive intermediate initiating a complex sequence of secondary reactions. Therefore, the halogen-substituted alkylsilicon compounds with a halogen atom at β-carbon are more appropriate for the isotope selective IR MPD since stable products are formed in the unimolecular decomposition of such molecules: halogenated silane and olefin molecules.

In this study we report the experimental investigation of the silicon isotope selective dissociation of $SiF_3C_2H_3Cl_2$ molecules induced by a pulsed TEA CO_2 laser irradiation. The dissociation of these molecules is expected to occur via the chlorine atom transfer from carbon to silicon:

$$SiF_3C_2H_3Cl_2 \rightarrow SiF_3Cl + C_2ClH_3 \qquad \text{(R.1)}$$

The only IR MPD products of $SiF_3C_2H_3Cl_2$ have been found to be chloroethylene and trifluorochlorosilane. The silicon isotope composition of the latter varies depending on the frequency of the laser radiation.

2 Experiment

$SiF_3C_2H_3Cl_2$ was synthesized from $SiCl_3C_2H_3$. At the first stage $SiCl_3C_2H_3$ was converted to $SiF_3C_2H_3$ using the reaction with SbF_3. Then, equal amounts of gaseous $SiF_3C_2H_3$ and Cl_2 were mixed in a glass vessel. After that, the mixture was exposed to weak UV light through quartz windows. The $SiF_3C_2H_3Cl_2$ was extracted from the reaction mixture using fractional condensation. The amount of the main impurity, SiF_4, did not exceed 1% of the amount of $SiF_3C_2H_3Cl_2$.

2.1 Radiation source

A tunable pulsed TEA CO_2-laser was used as a source of the IR radiation [26]. The maximum pulse energy of the laser was about 5 J. The laser beam was collimated in front of the input window of a reaction cell by an aperture of 1 cm in diameter. The energy of the laser radiation pulse was varied by changing the discharge energy and the laser cavity pressure. To change the pulse energy significantly, a set of parallel-sided CaF_2 plates was used. The average energy of the laser radiation was measured with an optical power meter in front of the cell and behind the cell. The unfocused uniform laser beam was used throughout all the experiments.

Typically the laser pulse has a 150-ns peak and a 1-μs nitrogen tail with approximately equal energies in the peak and in the tail. In some experiments we used a $CO_2/H_2/He$ laser mixture instead of the $CO_2/N_2/He$ mixture [26]. With this mixture, the tail of the laser pulse was with 300-ns significantly shorter and the energy of the tail was about 25% of the total energy.

2.2 Experimental

All the experiments have been carried out under the batch cell conditions, at room temperature. Samples of neat chloromethyltrifluorosilane with natural abundance of silicon isotopes were irradiated. The reaction cell was a Pyrex-glass cylinder with NaCl windows. The length of the reaction cell was 42 cm; the cell diameter was 3 cm. The cell

content was analyzed using a MH-1303 mass spectrometer. The cell was continuously connected to the ion source of the mass spectrometer through a glass pinhole of about 20 μm in diameter. Therefore, the cell content could be analyzed at any moment during the laser irradiation. The concentration and isotope composition of SiF_3CH_2Cl were determined from the $m/e = 132$–138 lines of the mass spectrum. The concentration and isotope composition of the SiF_3Cl MPD product were determined from the $m/e = 120$–124 lines of the mass spectrum. The isotope analysis of these species was hindered by the superposition of the mass spectra of the compounds containing different chlorine and silicon isotopes. To overcome this problem, a special software was developed to determine the composition of ^{35}Cl–^{37}Cl and ^{28}Si–^{29}Si–^{30}Si isotopes taking into account all the lines in the mass spectrum. The corresponding algorithm is described in Ref. [25].

IR spectra were measured with a Fourier-transform infrared (FTIR) spectrometer (Bruker Vector 22) with the spectral resolution of 1 cm^{-1}.

2.3 Computational details

Geometry calculations of the reactants, products, and intermediates were performed with the GAUSSIAN98 suit of programs [27]. Those were fully optimized and the fundamental frequencies were calculated using the density functional theory at the hybrid B3LYP level [28, 29] with the 6-31G(p,d) basis set and the unrestricted formalism for the case of radicals. Geometries of transition states (TS) were found using the QST2 procedure [30] and then optimized. The TS geometries were confirmed by frequency calculations of the same level of theory presenting one imaginary frequency corresponding to the transition vectors pointing in the direction of the reaction coordinate. The structures corresponding to the local minima (reactant and products) were as well confirmed through the frequency calculations, where all frequencies have to be necessarily real at local minima.

3 Results and discussion

3.1 Infrared spectrum

The most intensive bands in the IR spectrum of 1,2-dichloroethyltrifluorosilane are located in the region of 850–1020 cm^{-1}. The IR spectrum in this region is shown in Fig. 1.

The vibration frequencies of $SiF_3C_2H_3Cl_2$ were calculated using the B3LYP procedure. The frequencies are listed in the first column of Table 1. The region of 850–1020 cm^{-1} covers the ν_{15}–ν_{19} vibrations of $SiF_3C_2H_3Cl_2$. The expected relative intensities of these vibrations are shown in

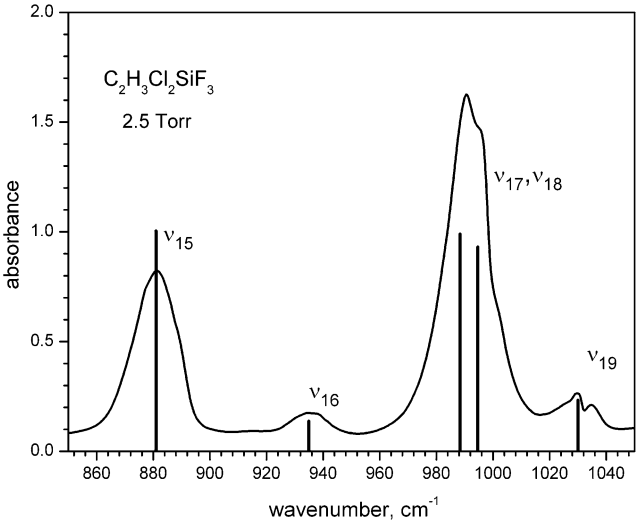

Fig. 1 FTIR spectrum of $SiF_3C_2H_3Cl_2$ in the spectral region of CO_2-laser radiation. Resolution 1 cm^{-1}, pressure 2.5 Torr, length of the reaction cell 18 cm. *Vertical lines* indicate the relative intensities of calculated vibration bands of the molecule

Fig. 1 by the vertical lines. According to the B3LYP procedure, the assignments of these bands are as follows: the band at $\nu_{15} = 881$ cm^{-1} corresponds to the symmetric stretch vibration of the SiF_3 group; the band at 990 cm^{-1} corresponds to two asymmetric stretch vibrations of the SiF_3 group ν_{17} and ν_{18}, which have slightly different frequencies. The weak bands at 935 and at 1030 cm^{-1} correspond to the rocking vibration of the CH_2 group ν_{16} and to the stretching vibrations of C–C bond ν_{19}. The latter band could partially overlap with the absorption band of the SiF_4 impurity.

The second column in Table 1 shows the isotopic shifts, the difference of the frequencies of $^{28}SiF_3C_2H_3Cl_2$ and $^{29}SiF_3C_2H_3Cl_2$. The frequencies of the molecules containing ^{29}Si and ^{28}Si were calculated using the same set of the force constants. The largest isotopic shifts are expected for Si–F asymmetric stretch vibrations ν_{17} and ν_{18}.

3.2 Infrared multiphoton absorption and dissociation

A few laser lines in the 10R branch of the CO_2 laser coincide with the strong bands ν_{17} and ν_{18} in the vicinity of 990 cm^{-1}. Figure 2 presents the dependence of $\langle n \rangle$—the average number of absorbed photons per molecule on the laser fluence measured at the 10R42 CO_2-laser line (992 cm^{-1}). One can see that the efficient multiphoton excitation of $SiF_3C_2H_3Cl_2$ is achievable even at essentially low laser fluences. The average number of absorbed photons per molecule reaches 15 at 0.5 J/cm^2. When the laser fluence is lower than 0.15 J/cm^2, the dependence is linear. The corresponding absorption cross section, derived from the slope of the liner dependence, was found to be 8.6×10^{-19} cm^2.

Figure 3 presents the dependence of the IR MPD probability β (an average probability of a single molecule to

Table 1 Experimental and calculated vibrational frequencies of $^{28}SiF_3C_2H_3Cl_2$ and calculated corresponding isotopical shifts for the ^{29}Si, ^{30}Si—substituted $SiF_3C_2H_3Cl_2$. Calculated vibrational frequencies for the transition state of reaction (R.1) are also shown

N	Calculated		Experimental	ν (TS), cm^{-1}
	$^{28}\nu$, cm^{-1}	$^{28}\nu$–$^{29}\nu$, cm^{-1}	ν, cm^{-1}	
1	28.2	−0.0002	–	$i \cdot 425.8$
2	81.2	0.0089	–	46.0
3	100.2	0.039	–	85.4
4	130.4	0.080	–	151.5
5	197.5	0.13	–	200.6
6	226.6	0.10	–	230.0
7	234.0	0.10	–	275.9
8	310.1	0.70	–	306.7
9	344.4	1.43	–	365.3
10	398.8	0.52	–	377.9
11	429.9	2.76	438	406.7
12	633.7	0.30	640	443.7
13	721.0	0.08	732	501.9
14	767.2	0.009	782	674.6
15	886.4	4.52	881	819.0
16	941.8	0.96	935	831.2
17	1006.4	8.74	991	841.3
18	1022.1	8.66	1030	929.6
19	1049.6	0.302	1126	982.0
20	1183.9	0.027	1169	1060.3
21	1199.1	0.57	1234	1109.7
22	1289.0	0.010	1273	1193.1
23	1352.1	0.019	1311	1302.7
24	1483.4	0	1441	1501.0
25	3092.5	0.0037	2958	3153.7
26	3101.2	0.0018	–	3175.7
27	3163.0	0.0064	–	3281.5

dissociate during a single laser pulse) on the laser fluence for $SiF_3C_2H_3Cl_2$ molecules. It was measured at the 10R(42) CO_2-laser line. The sample pressure was 0.3 Torr. For comparison, the same data for Si_2F_6 molecules [31] and SiF_3CH_2Cl [25, 32] are shown.

Apparently, $SiF_3CHClCH_2Cl$ molecules dissociate considerably easier than Si_2F_6 and SiF_3CH_2Cl. The dissociation rate is readily detectable even at fluences <0.1 J/cm^2. When the laser fluence is higher than 0.5 J/cm^2, more than half of the sample molecules dissociate within a single pulse of the laser radiation.

The mass spectrometric analysis of the reaction cell contents after the irradiation shows that the only products of dissociation are SiF_3Cl and C_2H_3Cl, and their concentrations are approximately equal. The product composition confirms that the dissociation proceeds via the Cl atom transfer from carbon to silicon (R.1).

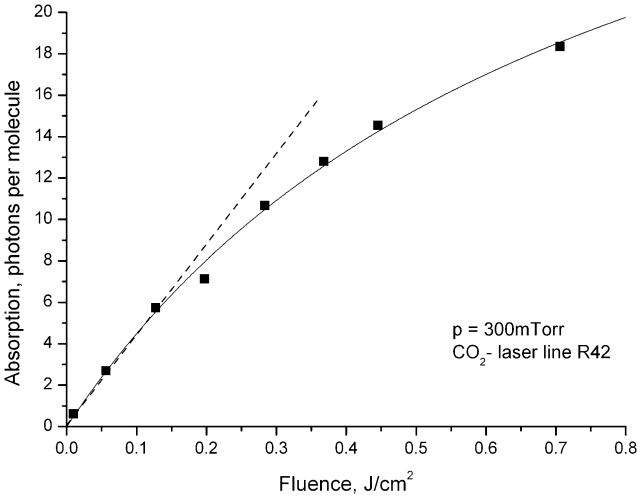

Fig. 2 Average number $\langle n \rangle$ of absorbed photons per molecule as a function of the laser fluence, measured at 10R(42) CO_2-laser line (992 cm^{-1}) at 300 mTorr sample pressure

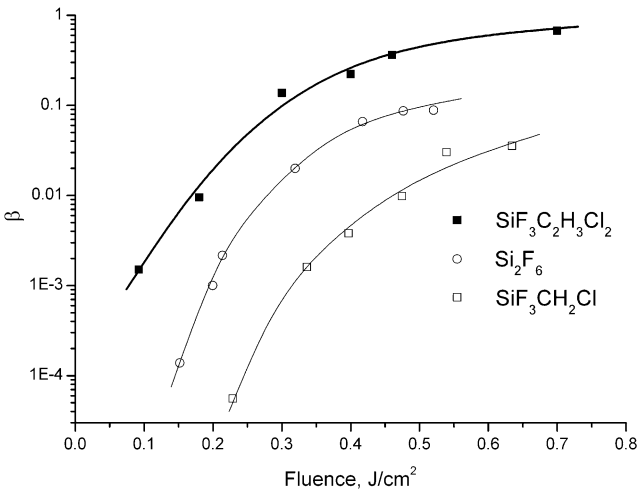

Fig. 3 Laser fluence dependence of the average probability β that a single $SiF_3C_2H_3Cl_2$ molecule dissociates during the single laser pulse, measured for the 10R(42) CO_2-laser line (992 cm^{-1}) at 300 mTorr sample pressure

Both products, SiF_3Cl and C_2H_3Cl, are stable molecules. They are gaseous at room temperature; but have different boiling points. The boiling points of the end products are lower than that of $SiF_3CHClCH_2Cl$. Thus, separation of the reaction mixture is easy to achieve using a low-temperature fractional condensation/evaporation procedure. For this purpose, the reaction mixture after irradiation was frozen in the glass appendix attached to the reaction cell, at liquid nitrogen temperature (−196°C) by immersing the appendix into liquid nitrogen. Then the liquid nitrogen was removed and the appendix was allowed to warm up slowly (∼0.05 K/s); the temperature and the pressure in the reaction cell were continuously recorded during the temperature rise. Figure 4 shows the corresponding pressure–temperature (P–T) dia-

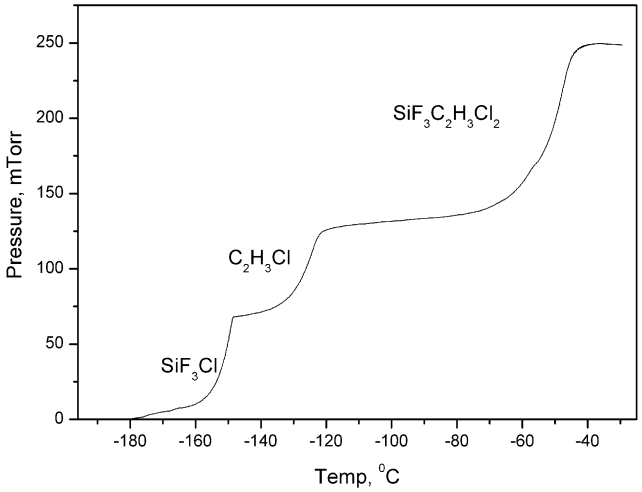

Fig. 4 Typical P–T diagram of the reaction mixture after irradiation

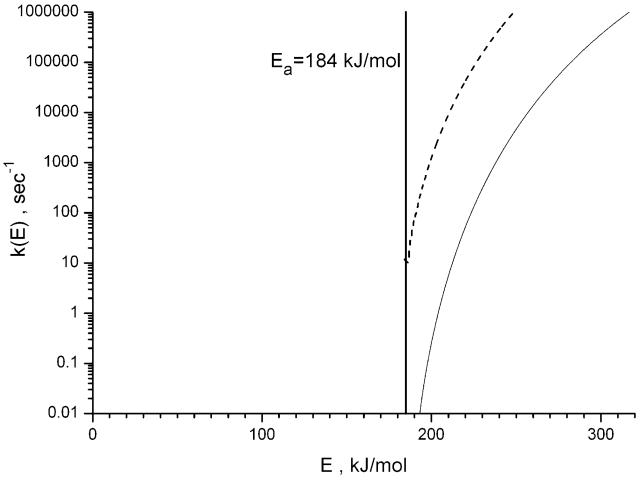

Fig. 5 Calculated vibrational energy dependence of the rate constant of the unimolecular decomposition of $SiF_3CHClCH_2Cl$ molecule using RRKM theory. The *vertical line* shows the dissociation energy of the molecule. *Dash line* shows the rate constant calculated using reduced set of molecular vibrations

gram of the reaction mixture of the dissociation products and the reagent $SiF_3CHClCH_2Cl$.

The concentration of each component of the gaseous mixture is associated with the height of the corresponding plateau in the diagram. The diagram confirms that the concentrations of the products SiF_3Cl and C_2H_3Cl are approximately equal. The vapor pressure of SiF_3Cl at $T = -145°C$ is about 0.1 Torr, while the vapor pressure of C_2H_3Cl and $SiF_3C_2H_3Cl_2$ is less than 0.01 Torr. Therefore, SiF_3Cl could be easily separated from the mixture at this temperature.

3.3 Calculated dissociation probability β

In the reaction of decomposition of $SiF_3CHClCH_2Cl$ to SiF_3Cl and C_2H_3Cl, the bonds Si–C and C–Cl are breaking while the Si–Cl bond is forming. The transition state parameters for this reaction were calculated using B3LYP method with the 6-31G(p,d) basis and the QST2 procedure. The transition state is rigid. The lengths of the breaking bonds in the transition state are 2.675 (Si–C) and 2.31 Å (C–Cl); which is much longer than their initial lengths (1.87 and 1.80 Å correspondingly). The length of the forming Si–C bond is 2.28 Å, which is close to the Si–C bond length in the SiF_3Cl molecule—2.024 Å. The calculated activation energy is 184 kJ/mol.

Also, the vibrational frequencies in the transition state have been calculated. They are shown in Table 1, column 4. RRKM calculations of the rate constant $k(E)$ of the unimolecular decomposition of $SiF_3CHClCH_2Cl$ have been performed using the activation energy and the vibrational frequencies from Table 1. A standard formula for RRKM calculations was used [33]:

$$k(E) = \frac{1}{h} \cdot \frac{W^{\neq}(E)}{\rho(E)}$$

The density of vibrational levels $\rho(E)$ of $SiF_3CHClCH_2Cl$ and the total number of vibrational levels of the transitional state $W^*(E)$ were numerically calculated using the direct enumeration method. The results are shown in Fig. 5. One can see from the figure that the molecule must be essentially overexcited vibrationally to be able to decompose within the laser pulse duration. The lifetime of the molecule becomes shorter than 1 μs only at energies >320 kJ/mol.

Using the RRKM calculations, the linkage could be established between the average number of absorbed laser radiation quanta $\langle n \rangle$ per molecule and the dissociation probability β, measured under the same experimental conditions, if the vibrational energy distribution function of the decomposing molecules is known. If it is not known; however, it could be assumed and then the assumption could be verified by comparing the calculations with the experimental data in Figs. 2 and 3. We have performed these calculations assuming that the distribution function over all vibrational modes is a Boltzmann distribution with a single vibrational temperature T_{vib}.

The Boltzmann distribution could be written as:

$$dn(E) = \rho(E) \frac{n_0}{Z_{\text{vib}}(T_{\text{vib}})} \exp\left(-\frac{E}{kT_{\text{vib}}}\right) dE \qquad (1)$$

where n_0 is the total initial concentration of the molecules, Z_{vib} is the vibrational partition function of the $SiF_3C_2H_3Cl_2$ molecule, $\rho(E)$ is the density of vibrational levels. Let us assume that the molecule dissociates, if it is excited up to energies higher than $E_a = 320$ kJ/mol. Hence, from (1)

we can link up the dissociation probability β and the average number of absorbed quanta per molecule $\langle n \rangle$:

$$\beta(T_{\text{vib}}) = \frac{1}{n_0} \int_{E_a}^{\infty} dn(E),$$
$$\langle n \rangle(T_{\text{vib}}) = \frac{1}{h\nu} \int_{0}^{\infty} E\, dn(E) \tag{2}$$

The vibrational frequencies of the $SiF_3CHClCH_2Cl$ molecule from Table 1 were used in the calculations. The density of the vibrational levels $\rho(E)$ was numerically calculated using the direct enumeration of all the vibrational levels of the molecule. The result of calculations is shown in Fig. 6 by the solid line. The solid squares present the experimental results, constructed using Figs. 2 and 3. One can see that the experimental dissociation probabilities are significantly higher than the calculated ones. Therefore, the assumption about Boltzmann energy distribution of the decomposing $SiF_3C_2H_3Cl_2$ molecules is not valid. In reality, the fraction of molecules which have enough energy to dissociate is much higher than it is predicted by the calculations. In the calculations, the assumption was made that all the 27 vibrational modes of the molecule have the same vibrational temperature. The mismatch between the experiment and the calculations might indicate that the vibrational modes of the excited molecule are not in total equilibrium.

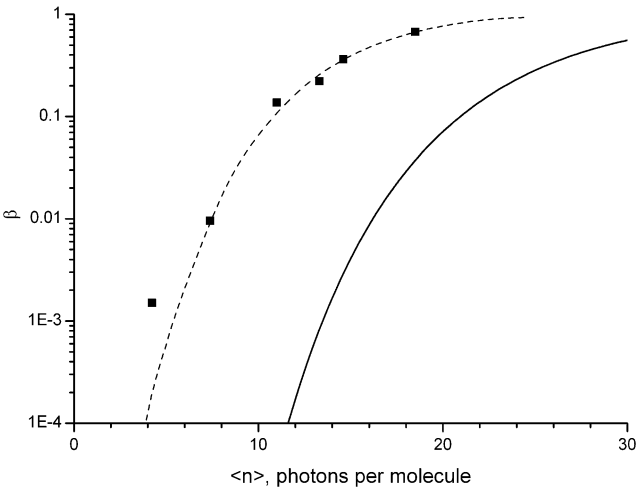

Fig. 6 Calculated probability $\beta(\langle n \rangle)$—*solid line*, and experimental $\beta(\langle n \rangle)$—*squares*. *Dash line* shows $\beta(\langle n \rangle)$ calculated using reduced set of molecular vibrations

This contradiction could be solved easily if expecting that not all vibrations of the molecule act in a laser excitation. To illustrate this we made calculations in assumption that four most low-frequency modes of the molecule do not participate in an energy redistribution. Dash line on Fig. 5 illustrates RRKM calculations of the rate constant $k(E)$ in such assumption. Corresponding calculations for dissociation probability are presented in Fig. 6 by dashed line. It was obvious that such simple method of the accounting of an intramolecular vibrational nonequilibrium is in a good agreement with the experimental results. Real distribution can not be obtained in such a simple way.

3.4 Isotope selective MPD of SiF_3CH_2Cl

Figure 7 shows the dependence of the MPD probability of the of $SiF_3C_2H_3Cl_2$ molecules on the wave number of the laser radiation—MPD spectrum (circlets). It was experimentally obtained by tuning the CO_2-laser radiation over the laser lines. Sample pressure was 0.3 Torr, the laser fluence was kept constant at about 0.4 J/cm^2 level. For comparison, the linear absorption IR spectrum of $SiF_3C_2H_3Cl_2$ in the spectral region in the vicinity of 10 μm is shown by the dashed curve.

The linear IR spectrum of $SiF_3C_2H_3Cl_2$ in the vicinity of 10 μ consists of several absorption bands, which partially overlap (Fig. 1). This could lower the efficiency of isotope separation. However, as one can see from Fig. 7, the MPD spectrum is essentially narrower than the linear spectrum.

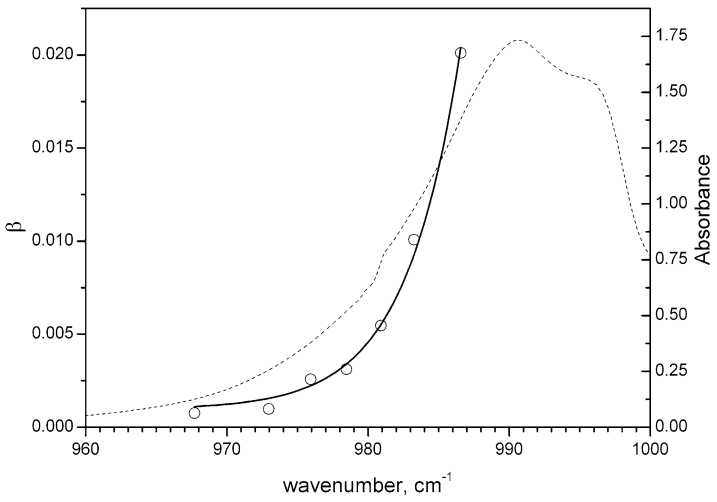

Fig. 7 Dependence of the probability of the MPD of $SiF_3CHClCH_2Cl$ molecules on the laser radiation wave number—MPD spectrum (*circles* and *solid line*). Sample pressure was 0.1 Torr, the laser fluence was kept constant at 0.4 J/cm^2. The *dashed curve* represents the FTIR spectrum

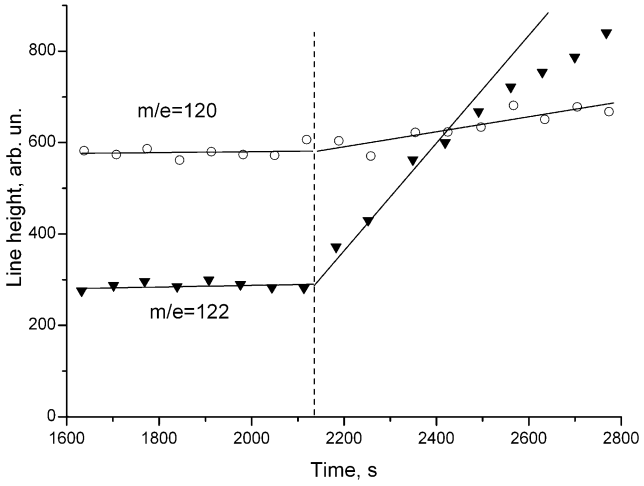

Fig. 8 Evolution of SiF_3Cl^+ mass-spectrometric line intensities during the irradiation of $SiF_3CHClCH_2Cl$. The laser radiation wave number was 956 cm^{-1}. The *vertical dashed line* indicates the moment when the laser was switched on

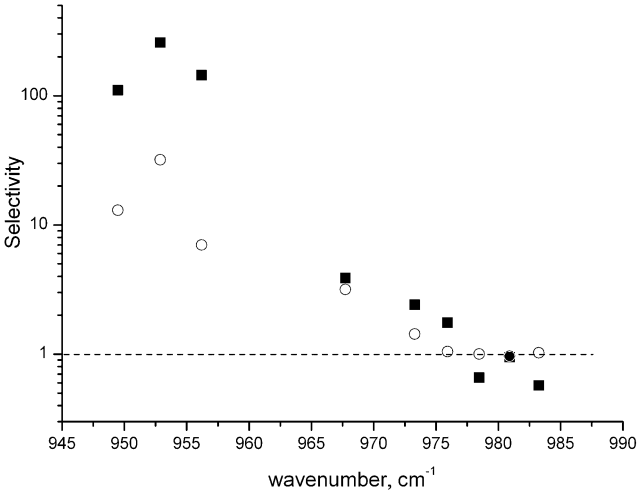

Fig. 9 Spectral dependences of the isotopic selectivities S_{30} and S_{29}. Pressure 0.3 Torr. *Solid squares*—S_{30}, *circles*—S_{29}

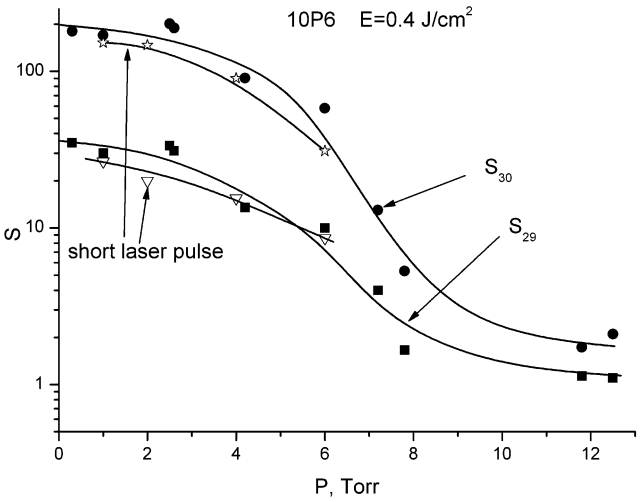

Fig. 10 Pressure dependence of S_{29}, S_{30} selectivities. Experiments using short laser pulses are represented with *stars* for S_{30} and *triangles* for S_{29}

The dissociation probability β changes by an order of magnitude, when the frequency of the laser radiation shifts by 16 cm^{-1}, the isotopic shift in the spectra of ^{28}Si and ^{30}Si isotopomers. Therefore, highly selective Si isotope separation by IR MPD is possible.

When the laser was tuned to the 10P branch ($\nu < 955$ cm^{-1}), we observed the preferred dissociation of those molecules with the rare silicon isotopes ^{29}Si and ^{30}Si. Figure 8 shows the example of the time dependence of the intensities of two lines of the SiF_3Cl mass spectrum during the laser irradiation. The line with $m/e = 120$ belongs to the $^{28}SiF_3^{35}Cl^+$ ions, and the line with $m/e = 122$ belongs to the $^{30}SiF_3^{35}Cl^+$ and $^{28}SiF_3^{37}Cl^+$ ions. The growth rate of the line with $m/e = 122$ line is roughly five times higher than that of the line with $m/e = 120$. Taking into account the natural abundances of silicon isotopes in the reagent, namely, 92.27% for ^{28}Si and 3.05% for ^{30}Si, we can estimate the relative rate of dissociation of ^{30}Si-containing molecules to be at least 150 times higher than the relative rate of ^{28}Si-containing molecules.

The ratio of the first order rate constant was used as a measure of the isotopic selectivity.

$$S_{30} = k^{30}/k^{28}, \qquad S_{29} = k^{29}/k^{28} \tag{3}$$

The effective dissociation rate constants k^{28}, k^{29}, and k^{30} were determined from the growth of the concentrations of products $^{28}SiF_3Cl$, $^{29}SiF_3Cl$, and $^{30}SiF_3Cl$. These concentrations were obtained from the $m/e = 120$–124 lines of the mass spectrum by solving the set of linear equations.

Using the linear approximation we obtain:

$$S_{30} = \frac{k^{30}}{k^{28}} = \frac{w_{30}/n_0^{30}}{w_{28}/n_0^{28}}, \qquad S_{29} = \frac{k^{29}}{k^{28}} = \frac{w_{29}/n_0^{29}}{w_{28}/n_0^{28}} \tag{4}$$

where $w_{30} = d[^{30}SiF_3Cl]/dt$ is the rate of $^{30}SiF_3Cl$ formation, w_{28} is the rate of $^{28}SiF_3Cl$ formation, and w_{29} is the rate of $^{29}SiF_3Cl$ formation; n_0^i is the initial concentration of $^iSiF_3C_2H_3Cl_2$, $i = 28, 29, 30$.

Figure 9 presents the spectral dependences of the isotopic selectivities S_{30} and S_{29} which have been obtained by tuning the CO_2-laser radiation over different rotational laser lines. The region 957–967 cm^{-1} corresponds to the gap between the 10P and 10R branches. All experimental points in Fig. 9 were obtained at a $SiF_3C_2H_3Cl_2$ pressure of 0.3 Torr.

Pressure dependence of the isotopic selectivity was measured at $\nu = 952.9$ cm^{-1}. The results are presented in Fig. 10. It was found that the isotopic selectivity stays essentially high over quite a large range of $SiF_3C_2H_3Cl_2$ pressure of up to 5–6 Torr. It drops down sharply for higher pres-

sure. The S_{30} decreases by about 10 times when the pressure changes from 6 to 8 Torr (Fig. 10).

Bagratashvili et al. have shown that the isotopical selectivity decreases due to intermolecular transfer of vibrational energy within the laser pulse duration [34]. If this were correct, then we should expect the selectivity to decrease slower when using shorter laser pulses. To shorten the CO_2-laser pulses, we have conducted the experiments using a $CO_2/H_2/He$ laser, which produces shorter pulses. The results are presented in Fig. 10 with stars for S_{30} and triangles for S_{29}.

One can see from Fig. 10 that the isotopical selectivity has *not* increased and its dependence on pressure has *not* changed significantly upon shortening the laser pulses. However, the IR MPD probability has increased for the same laser fluences.

This independence of the isotopical selectivity on the laser pulse duration in our experiments is unexpected and contradicts the current view on significance of intermolecular energy transfer in isotope-selective MPD. We have applied the kinetic model developed by Bagratashvili et al. [34] to describe our experimental results. It was found that this kinetic model is unable to explain the sharp drop in the pressure dependence of the isotopic selectivity. The S_{30} selectivity drops tenfold when the pressure increases from 5 to 8 Torr. We could not simulate such a sharp drop at any values of the model parameters.

The most probable reason for this sharp selectivity decrease could be the presence of thermal decomposition processes of $SiF_3C_2H_3Cl_2$, the contribution of which increases with pressure.

4 Conclusion

The main products of the $SiF_3C_2H_3Cl_2$ IR MPD are stable molecules SiF_3Cl and C_2H_3Cl. The maximum selectivity reached for ^{30}Si in our experiments was as high as 240, which is significantly higher than that for Si_2F_6, the molecule for which the IR MPD was considered as a base for the laser technology of silicon isotope separation. High selectivity for ^{29}Si has been achieved ($\sim$35). In all the previous studies, ^{29}Si could not be enriched at any significant level [4–19, 25]

Isotopic selectivity remains essentially high up to 5 Torr pressure. Current research confirms the previous assumption that the silicon organic molecules with β-chlorine or fluorine atoms should demonstrate the efficient multiphoton dissociation and the high silicon isotope selectivities [25].

Acknowledgements This work was supported by the Russian Foundation for Basic Research (grant No. 09-03-00868-a) and by the Siberian Branch of the Russian Academy of Sciences (grant No. 52/2009).

References

1. T. Ruf, R.W. Henn, M. Asen-Palmer, E. Gmelin, M. Cardona, H.J. Pohl, G.G. Devyatych, P.G. Sennikov, Solid State Commun. **115**, 243 (2000)
2. R.K. Kremer, K. Graf, M. Cardona, G.G. Devyatykh, A.V. Gusev, A.M. Gibin, A.V. Inyushkin, A.N. Taldenkov, H.-J. Pohl, Solid State Commun. **131**, 499 (2000)
3. ed. by D.R. Lide, *CRC Handbook of Chemistry and Physics*, 79th edn. (CRC Press, Boca Raton, 1998)
4. J.L. Lyman, S.D. Rockwood, J. Appl. Phys. **47**, 595–601 (1976)
5. N.K. Serdyuk, E.N. Chesnokov, V.N. Panfilov, React. Kinet. Catal. Lett. **17**, 19 (1981)
6. M. Kamioka, S. Arai, Y. Ishikawa, S. Isomura, N. Takamiya, Chem. Phys. Lett. **119**, 357–360 (1985)
7. M. Kamioka, Y. Ishikawa, H. Kaetsu, S. Isomura, S. Arai, J. Phys. Chem. **90**, 5727–5730 (1986)
8. H. Suzuki, H. Araki, T. Noda, J. Jpn. Instrum. Methods **61**, 145 (1997)
9. J.L. Lyman, B.E. Newman, T. Noda, H. Suzuki, J. Phys. Chem. A **103**, 4227–4232 (1999)
10. S. Arai, H. Kaetsu, S. Isomura, Appl. Phys. B **53**, 199–202 (1991)
11. M. Polianski, O.V. Boyarkin, T.R. Rizzo, V.M. Apatin, V.B. Laptev, E.A. Ryabov, J. Phys. Chem. A **107**, 8578–8583 (2003)
12. S.R. Gorelik, E.N. Chesnokov, L.V. Kuibida, R.R. Akberdin, A.K. Petrov, Appl. Phys. B **78**, 119–125 (2004)
13. A.K. Petrov, A.V. Chernyshev, E.N. Chesnokov, S.R. Gorelik, L.V. Kuibida, K. Nomaru, H. Kuroda, Dokl. Akad. Nauk **385**(5), 638 (2002) (in Russian)
14. A.V. Chernyshev, K. Nomaru, A.K. Petrov, E.N. Chesnokov, S.R. Gorelik, L.V. Kuibida, R.R. Akberdin, H. Kuroda, J. Phys. Chem. A **107**(44), 9362–9367 (2003)
15. P.V. Koshlyakov, E.N. Chesnokov, S.R. Gorelik, A.K. Petrov, Russ. J. Phys. Chem. B **25**(5), 22 (2006)
16. S.S. Alimpiev, A.M. Velichko, S.M. Nikiforov, G.L. Odobashyan, B.G. Sartakov, S.V. Sin'ko, Pis'ma Zh. Tekhn. Fiz. **14**, 1786 (1988) (in Russian)
17. P.V. Koshliakov, S.R. Gorelik, E.N. Chesnokov, A.V. Vorobiev, A.K. Petrov, Appl. Phys. B **84**, 529 (2006)
18. V.B. Laptev, L.M. Tumanova, E.A. Ryabov, High Energy Chem. **32**, 108 (1998) (in Russian)
19. V.Y. Baranov, A.P. Dyad'kin, V.A. Kuz'menko, J. Quantum Electron. **20**, 450 (1990) (in Russian)
20. G. Fishwick, R.N. Haszeldine, C. Parkinson, P.J. Robinson, R.F. Simmons, J. Chem. Soc., Chem. Commun., 382 (1965)
21. W.I. Bevan, R.N. Haszeldine, J. Middleton, A.E. Tipping, J. Organomet. Chem. **23**, 17 (1970)
22. R.N. Haszeldine, P.J. Robinson, R.F. Simmons, J. Chem. Soc. B, 1357 (1967)
23. R.N. Haszeldine, P.J. Robinson, R.F. Simmons, J. Chem. Soc. B, 1890 (1964)
24. D. Graham, R.N. Haszeldine, P.J. Robinson, J. Chem. Soc. B, 611 (1971)
25. P.V. Koshlyakov, S.R. Gorelik, E.N. Chesnokov, O.S. Aseev, A.A. Rakhymzhan, A.K. Petrov, Photochem. Photobiol. (2009). doi:10.1111/j.1751-1097.2009.00541.x
26. M.V. Ivashchenko, A.I. Karapuzikov, I.V. Sherstov, J. Quantum Electron. **31**(11), 965–969 (2001) (in Russian)
27. M.J. Frisch G, W. Trucks, H.B. Schlegel, G.E. Scuseria, M.A. Robb, J.R. Cheeseman, V.G. Zakrzewski, J.A. Montgomery Jr., R.E. Stratmann, J.C. Burant, S. Dapprich, J.M. Millam, A.D. Daniels, K.N. Kudin, M.C. Strain, O. Farkas, J. Tomasi, V. Barone, M. Cossi, R. Cammi, B. Mennucci, C. Pomelli, C. Adamo, S. Clifford, J. Ochterski, G.A. Petersson, P.Y. Ayala, Q. Cui, K. Morokuma, D.K. Malick, A.D. Rabuck, K. Raghavachari, J.B. Foresman, J. Cioslowski, J.V. Ortiz, A.G. Baboul, B.B. Stefanov, G. Liu,

A. Liashenko, P. Piskorz, I. Komaromi, R. Gomperts, R.L. Martin, D.J. Fox, T. Keith, M.A. Al-Laham, C.Y. Peng, A. Nanayakkara, C. Gonzalez, M. Challacombe, P.M.W. Gill, B.G. Johnson, W. Chen, M.W. Wong, J.L. Andres, M. Head-Gordon, E.S. Replogle, J.A. Pople, *Revision A. 6–A. 11* (Gaussian Inc., Pittsburgh, 1998)

28. A.D. Becke, J. Chem. Phys. **98**, 5648 (1993)
29. C. Lee, W. Yang, R.G. Parr, Phys. Rev. B **37**, 785 (1988)
30. L.A. Curtiss, K. Raghavachari, G.W. Trucks, J.A. Pople, J. Chem. Phys. **94**, 7221 (1991)
31. H. Okamura, V. Tosa, T. Ishii, K. Takeuchi, J. Photochem. Photobiol. A **95**, 203–207 (1996)
32. P.V. Koshliakov, S.R. Gorelik, E.N. Chesnokov, A.V. Vorobiev, A.A. Rakhymzhan, A.K. Petrov, Dokl. Akad. Nauk **415**(5), 1–4 (2007) (in Russian)
33. P.J. Robinson, K.A. Holbrook, *Unimolecular Reactions* (Wiley, New York, 1972)
34. V.N. Bagratashvili, V.S. Doljikov, V.S. Letokhov, E.A. Ryabov, Appl. Phys. **20**, 231–235 (1979)